ACOUSTIC FLIGHT TEST OF THE EC130 B4 IN THE SCOPE OF THE FRIENDCOPTER PROJECT

H.-J. Marze
henri.marze@eurocopter.com

M. Gervais
marc.gervais@eurocopter.com

P. Martin
pierre.martin@eurocopter.com

P. Dupont
pierre.dupont@eurocopter.com

EUROCOPTER
Aéroport International Marseille-Provence
13725 Marignane, FRANCE

Abstract: An extensive noise abatement flight test was performed on the EC130 B4 aircraft, with noise data gathered on large linear and rectangular arrays on the ground. The main objectives of the flight test were to build an acoustic database for the aircraft, and to evaluate flight test and data analysis methodologies used in noise abatement testing.

A large matrix of flight conditions was tested, including level flight, descent, climb, deceleration/acceleration, hover, ground idle and turning flight. In addition, manoeuvring flight segments corresponding to different unsteady phases of a typical flight were performed. In all, approximately 150 flights were recorded in two separate campaigns.

A novel methodology is introduced to acquire manoeuvring data and reconstruct footprints for complete flight profiles. This methodology provides a way to reduce flight test costs while emphasising the acquisition of data corresponding to realistic flight manoeuvres. The resulting database can be used to systematically design low-noise flight procedures.

1. INTRODUCTION

Civil helicopters serve many useful functions in the public spheres. These include emergency medical service, search-and-rescue operations, law enforcement missions, and passenger transport. Their ability to takeoff and land from remote areas and unprepared terrain allow them to fulfil their mission with a high degree of flexibility. On the other hand, this unique capability means that rotorcraft typically fly in close proximity to populated communities, which are therefore exposed to noise.

Throughout the years, the rotorcraft industry has made great strides in reducing the level and annoyance of noise sources on helicopters. Every effort is now made to include the latest noise reduction features on new aircraft (see [1]). Noise abatement flight procedures are another means of reducing rotorcraft noise, and they have been shown experimentally and theoretically to have significant potential (see for example [2]-[8]). These procedures require

no design change to the aircraft, and can therefore be used on older models without the need for a retrofit, or they can help further reduce operational noise on modern designs.

One of the main obstacles to the further development of noise abatement procedures is the complexity associated with the acoustic data gathering and analysis methodologies. Indeed, the steady and unsteady flight procedures that can be used for noise abatement are varied and usually occur over a large ground area during a typical flight. This requires advanced flight test and analysis techniques, different from what is used in acoustic certifications performed according to ICAO or FAA standards ([9] and [10]). At the same time, a high level of accuracy and repeatability is desired, and the costs must be maintained at a viable level.

In response to the increased importance of helicopter operational noise, ICAO has recently published guidance material relating to the provision of land use planning data (see Attachment H of [9] and Appendix 9 of [11]). At the present time, information is still being gathered and analysed in order to provide further guidance material. This paper will provide some insight into the complexities and possible implementation methodologies of noise abatement and land use planning flight testing.

This paper will first introduce the aircraft and present a detailed description of the extensive test means that were deployed. The full test matrix will be presented before showing sample acoustic results illustrating the main findings, for steady-state and manoeuvring flights.

1.1   Friendcopter project

Friendcopter, launched in 2004, is a project partially funded by the European Union with a goal of improving the environmental acceptance of helicopters. The technical aspects of the 4.5-year project are divided in four main workpackages (WP): WP2 – Noise Abatement Flight Procedures, WP3 – Engine Noise Reduction, WP4 – Cabin Noise Reduction, and WP5 – Rotor Noise Control (sample Friendcopter publications can be found in [12] and [13]).

This paper focuses on the noise abatement aspect of the project, and more particularly on the acoustic flight test that was performed using the EC130 B4 aircraft. Flight tests of the A109 and EC135 are also part of the Friendcopter project, however they are outside the scope of this paper.

The objectives of the EC130 B4 flight test were:
▪ to improve flight test and data analysis procedures used to obtain acoustic footprints, for the various phases of civil helicopter flight,
▪ to guide the development of a methodology to design low noise flight procedures. The goal of these flight profiles is to reduce the level and extent of acoustic footprints for a given aircraft, and to be adaptable to various noise-sensitive areas,
▪ to expand existing acoustic/performance databases in order to gain additional knowledge on the generation and propagation of rotorcraft noise, useful for the design of noise abatement procedures. The data collected in this flight test will serve to enrich the database contained in the rotorcraft noise footprint tool being developed as part of Friendcopter (HELENA – HELicoper Environmental Noise Analysis).

2. AIRCRAFT DESCRIPTION

The EC130 B4 is a light single-engine helicopter incorporating a three-bladed main rotor and a modulated Fenestron® anti-torque system. The aircraft tested was a production-configured model, and the test gross weight was between 2300 kg and 2580 kg. Typical configurations for this aircraft include 7 or 8 passenger seats. The level flight airspeed for minimum engine torque at maximum continuous power (V_H) for this aircraft is 126 knots, and the best rate-of-climb airspeed (V_y) is 70 knots.

The rotor RPM is automatically controlled by the engine FADEC as a function of airspeed and altitude for noise reduction purposes. The normal rotor operating speed at sea level pressure altitude and within a range of airspeed between V_y and V_H is 386 RPM.

Figure 1 shows a picture of a helicopter representative of the one tested during the Friendcopter trials.

Figure 1. EC130 B4

It is important to take into account the flight envelope limits in the design of noise abatement procedures. Figure 2 presents the height-velocity diagram for the EC130 B4, which shows the combination of height and airspeed that must be avoided for this single engine aircraft. Particular care must be taken to respect the limits during the initial phase of a takeoff and final phase of an approach. This can often limit the potential benefits of optimal noise abatement procedures.
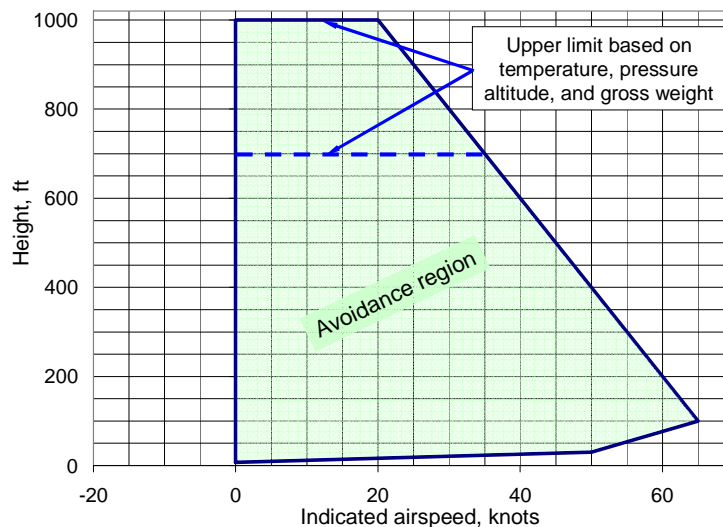
Figure 2. Height-velocity diagram for EC130 B4

3

3. TEST SETUP

3.1.   Acoustic data acquisition & processing

The basic system used to acquire acoustic data is composed of a number of 3-channel measurement stations (see Figure 3). Each station digitally records the noise at a sampling rate of 65356 hertz and performs a 1/3-octave analysis of the signal in real-time. The 1/3-octave results are transmitted through WI-FI to a central acoustics analysis station.

The 1/3-octave analysis is computed in real-time every 0.5 seconds in accordance with the ICAO Annex 16 specifications, with a SLOW time weighting approximation based on the four term exponential approximation contained in Annex 16.
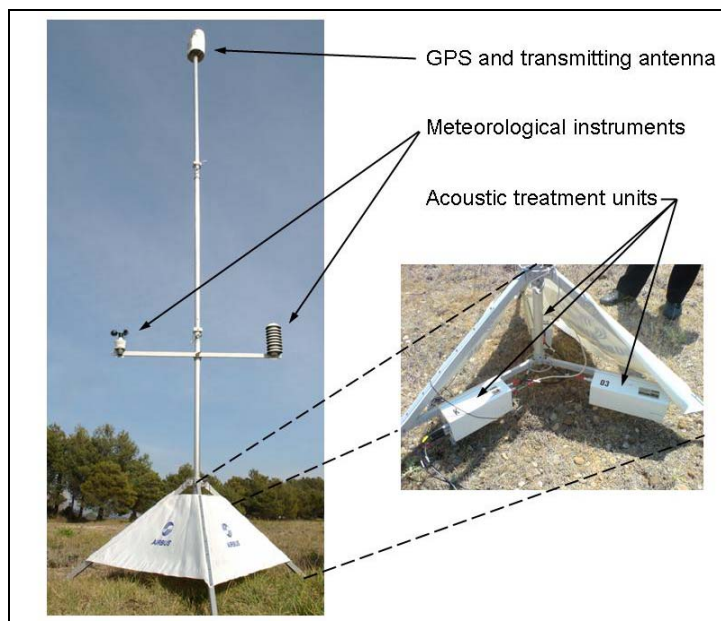
Figure 3. Acoustic measurement station, with 3 acoustic treatment units (each 1 channel)

The analysis station receives real-time data from each measuring station, which allows online monitoring of the 1/3-octaves for each run and each microphone. The acoustic pressure signal is stored on a local hard drive at each measurement station and downloaded to the central computer after each day of testing. The measurement stations also incorporate some meteorological instrumentation, for temperature, humidity, and wind data acquisition, however this capability was not used in the tests described herein (the meteorological system used is described in more detail in a following section).

Each microphone is calibrated using a pistonphone signal, and the measurement software automatically calibrates the subsequent recorded signals using the calibration value. A pink noise signal is also recorded for post-processing corrections of the frequency content. Ambient noise levels are recorded as well.

The post-processing corrections applied to the 1/3-octaves were: microphone frequency response, measurement system frequency response (pink noise), free-field insertion loss of windscreen, free-field directional response, and background noise correction.

In most cases, pressure-field microphones that offer a nearly flat frequency response at frequencies up to 20 kHz were used. After initial analysis of the results, it was decided during the campaign to use diffuse-field on some lateral microphones. This was done in order to allow for a dynamic range which covers lower dB values, since the noise of the helicopter was very low in some conditions on far away lateral microphones. The diffuse-field microphones that were used have a nearly flat frequency response up to 10 kHz.

3.2.   Microphone installation

Two main configurations of the measurement installation were used; a rectangular grid array of 36 measurement points, and a linear array of 9 or 11 measurement points. The grid array was mostly used for manoeuvring flight conditions, while the linear array was used for steady-state conditions.

The following figure show the position of the measurement points on the test site (an airfield called 'La Fare Les Oliviers' near the Eurocopter plant in Marignane, France) for the test campaigns held in June and September 2006).

Figure 4. Microphone linear and grid arrays

Two types of microphone setups were used; inverted ground plane microphones, and certification-type 1.2m-height microphones (both setups were installed as per [9]). Figure 5 shows both setups as installed during the flight tests. The primary setup specified for the Friendcopter test was the ground plane microphone, since it mostly eliminates the effects of ground reflections and thus facilitates the data analysis. However, since most data already available on existing helicopters was gathered in the frame of acoustic certification (with

1.2m-height microphones), it was judged interesting to also record data with this alternative setup. Therefore, the flights done during the September campaign (linear array) were all performed with both microphone setups recording simultaneously. The 1.2m-height microphones are installed in a grazing incidence fashion with respect to a point 150 m above the centreline microphone. All results presented in this paper were derived from data gathered on inverted ground plane microphones.

Figure 5. Microphone installation, showing 1.2m-height and ground plane microphones

3.3.   Trajectory and aircraft flight parameters

The following table lists the parameters that were recorded for each flight.

Table 1. List of recorded trajectory and aircraft performance parameters

Parameter	Comment
Position in local coordinates	Computed at the rotor hub. Origin: GPS*
True airspeed	Indicated airspeed (IAS) with correction from flight manual
Ground speed	Speed in the local coordinate system. Origin: GPS*
Pitch, Roll, Yaw	Origin: Attitude Heading Reference System (AHRS)
Static Pressure	Origin: Vehicle & Engine Multifunction Display (VEMD)
Pressure Altitude	Origin: VEMD
External Temperature	Origin: VEMD
Main Rotor RPM	Origin: Fully Automated Digital Electronic Control (FADEC)
Gas Turbine Generator	Origin: FADEC
Engine Torque	Origin: FADEC
Mass	Computed based on aircraft weight, ballast, and VEMD
Lateral, longitudinal, collective, pedal positions	Origin: gauges installed for the tests

* The GPS data was post-processed in differential mode.

A display was installed onboard the aircraft in order to provide trajectory and airspeed guidance to the pilot. This DGPS system ensured the repeatability of trajectories. In this system, the pilot is shown an anticipated indication of the target aircraft position on the display, as well as the associated lateral and vertical tolerances. The trajectory drift can therefore be corrected smoothly by the pilot, which avoids impulsive increases in noise that can result from quick pilot corrective inputs. The flight test engineer onboard the aircraft can review the validity of each run on the display after the flight. All the flight profiles to be tested are pre-programmed in the system and can be easily selected by the crew.

3.4. Meteorological data acquisition

The following meteorological parameters were measured at a point 10 meters above the ground: wind speed (knots), wind direction (degrees), relative humidity (%), atmospheric pressure (kPa), and temperature (°C).

In addition, the temperature and atmospheric pressure were measured at the flight altitude using the aircraft onboard instruments. The groundspeed derived from the GPS reading was also used to compute the head/tailwind at the flight altitude.

4. TEST MATRIX

The two test campaigns were designed to fully characterize the acoustics of the EC130 B4 throughout its normal flight envelope. As such, the test matrix is very extensive, and includes steady-state, manoeuvring, hover and ground run measurements. For the sake of brevity, hover and ground run results will not be discussed in this paper, and neither will turns nor accelerations/decelerations.

The following table shows the steady-state test matrix. The flight conditions include flyovers at airspeeds up to V_H, and takeoffs and approaches at various airspeeds and glideslopes (from maximum continuous power climbs to 14.5° descents).

Table 2. Steady-state flight test matrix

	Glideslope\ TAS	58 kt	V_Y 70 kt	80 kt	95 kt	0.9 V_H 113.4 kt	V_H 126 kt
Takeoff	**Max Continuous Power (MCP)**	X	X				
	Slope: +9°	X	X				
	+6°	X	X	X	X		
	+3°	X	X	X	X	X	
Flyover	**0°**	X	X	X	X	X	X
Approach	**Slope: -2°**	X	X	X	X	X	
	-4°	X	X	X	X		
	-6°	X	X	X	X		
	-8°	X	X	X	X		
	-10°	X	X	X	X		
	-12°	X	X				
	-14.5°	X					
IGE Hover	**2m height**	Measurements from 45° to 360° in 45° increments around the aircraft					
Ground Idle	**100%Nr, minimum collective**	Measurement from 45° to 360° in 45° increments around the aircraft					

Manoeuvres are important in terms of acoustics since they make-up the transition phases between steady-state flight conditions. In fact the steady-state approach and takeoff phases represent relatively short segments of a typical flight. In addition, accelerations and decelerations have been shown to have a powerful impact on the noise during descent, and can be used judiciously as part of a noise abatement approach profile [6].

In this research, it was decided to systematically study each of the individual steady-state and manoeuvring phases of a typical flight. Segments that were of particular interest were the transitions between hover/climb, climb/flyover, flyover/approach, and approach/hover. The advantage of this procedure is that the resulting database can then be used to piece together a

wide variety of segments to obtain the complete desired flight, without neglecting the unsteady transition segments. Also, since the individual flight segments are fairly short, the size of the required microphone array is shorter than the one needed when complete flights are flown (which can extend over a few kilometres). This methodology is further developed in the results section of this paper. The following table shows the matrix of manoeuvring flights that were achieved.

Table 3. Manoeuvring flight test matrix

Procedure	
Bank Turn	15° bank turn at 70 kt, 25° bank turn at 100 kt
Climb	Start and end of normal takeoff
	Start and end of low noise takeoff
Landing	Start and end of normal approach
	Start and end of low noise approach
	Start and end of low noise approach (alternate)
Acceleration and Deceleration	Level flight acceleration and deceleration
	Natural climb deceleration

5. SAMPLE RESULTS

5.1. Steady-state flights

Figure 6 shows the lateral distribution of the maximum A-weighted sound pressure level for the case of a level flyover at 90 knots. As discussed above, 11 microphones are used, covering 600 meters to each side of the helicopter. On the figure, the main rotor advancing side (port) corresponds to positive Y values.
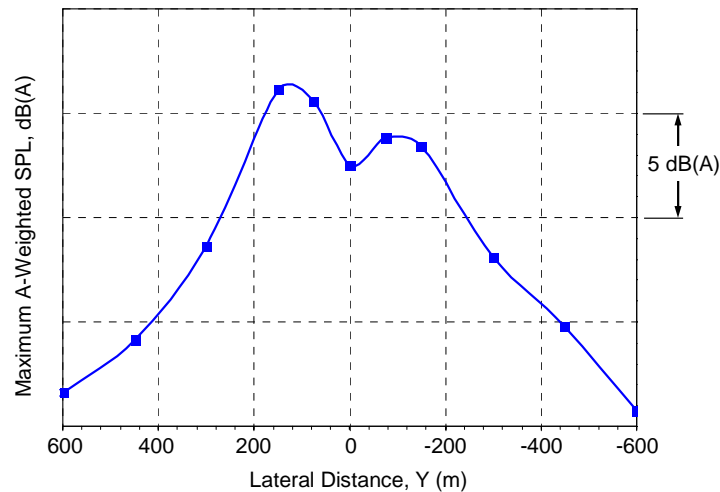
Figure 6. Maximum A-weighted sound pressure level as a function of lateral distance

Two main observations can be made regarding the figure above, which is similar in shape to flyovers at other airspeeds. First, the lateral directivity is highly unsymmetrical. This is due to the non-symmetrical nature of the two principal noise sources: the main rotor and the Fenestron®. Second, the typical 'bell-curve' exhibited by some helicopter is not reproduced on this helicopter, due primarily to the shielding effect of the Fenestron®. Therefore, the lateral distribution of the microphones required to accurately represent the characteristics of this aircraft is critical. Indeed, it is readily observed that a minimum of 7 microphones are needed; from -300 meters to +300 meters. Deriving data for land use planning using fewer

microphones appears erroneous in this case. The levels at lateral distances over 300 meters seem to decay in the typical manner, which indicates that it may not be necessary to position microphones past 300 meters. However, long distance propagation at near-grazing incidence angles is still a subject of active research, and measurements at far lateral distances are highly influenced by ambient noise, terrain absorption properties, and the helicopter acoustic levels. For example, small helicopters tend to have very low levels at 600 meters, hence it might not be useful to gather data at such distance for these aircraft. The acquisition of noise data at microphones beyond 300 meters is therefore subject to further study and must be evaluated on a case-by-case basis.

In terms of noise abatement applications, an interesting means of data representation is the so-called 'fried-egg' plot (the rate-of-descent/climb as a function of airspeed). Such a plot can be used to identify high noise regions within the steady-state operational envelope for a given aircraft. Figure 7 shows the maximum A-weighted sound pressure level measured at the centreline microphone for a range of airspeeds and rates-of-descent/climb. Multiple flights at the same flight condition were averaged. The true airspeed is used, and lines are shown representing the corresponding aerodynamic flight path angles (γ). Note that absolute values of the noise levels are not shown (contour lines are 1 dB(A) apart).
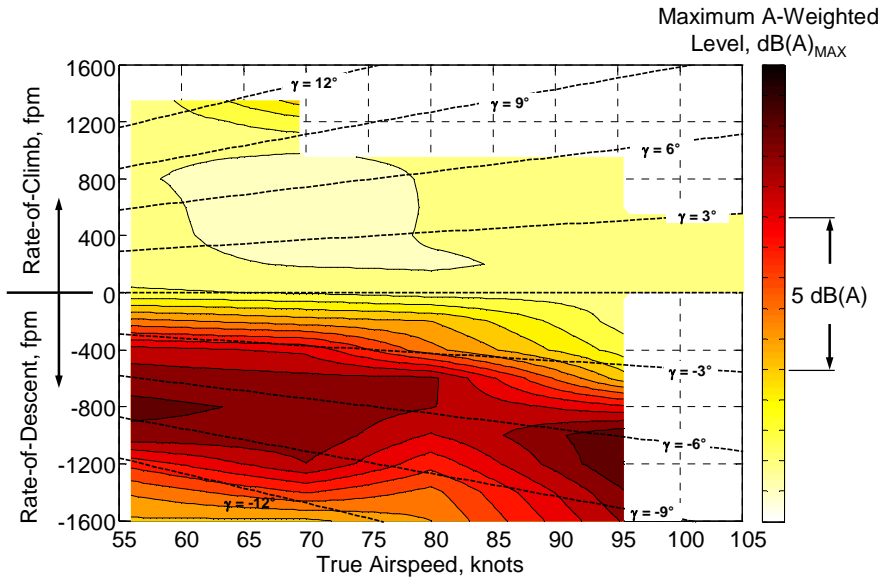
Figure 7. Maximum A-weighted sound pressure level at the centre microphone as a function of true airspeed and rate-of-descent/climb (contour lines are 1 dB(A) apart)

Figure 7 clearly highlights the high-noise regions within the helicopters flight envelope, as measured at the centreline microphone position during steady-state flight. For this aircraft and flight configuration, these high-noise regions are located between 6° and 9° descent angles at airspeed ranges between 55 and 70 knots, and also above 90 knots. The low-noise regions are also made apparent through this figure. The low airspeed/high rate-of-descent region corresponds to a low-noise approach (7 dB(A) below the high-noise descent region), and the low-noise takeoff region covers a fairly wide envelope between 3° and 9° at airspeeds between 60 and 80 knots. Also note that there is a 15 dB(A)$_{MAX}$ difference between the highest noise region and lowest noise region of the entire steady-state flight envelope. This emphasises the importance of noise abatement procedures in the general objective of rotorcraft noise reduction.

It is important to note that an acceleration or deceleration along a particular flight path angle has an important effect on the conclusions that can be made regarding Figure 7. As discussed in [6], a deceleration has approximately the same first order effect on the noise than a change in flight path angle. Winds also play a significant role in the noise generation and propagation during approach [14]. These factors, although outside the scope of this paper, have to be taken into account in order to design practical noise abatement procedures.

In order to fully assess the relative acoustic merit of various flight profiles, it is important to consider both the level and duration of a noise event. The next figure shows the sound exposure level (SEL) plot of airspeed vs. rate-of-descent/climb. The SEL is a common integrated noise metric, and its formulation is described in [9].
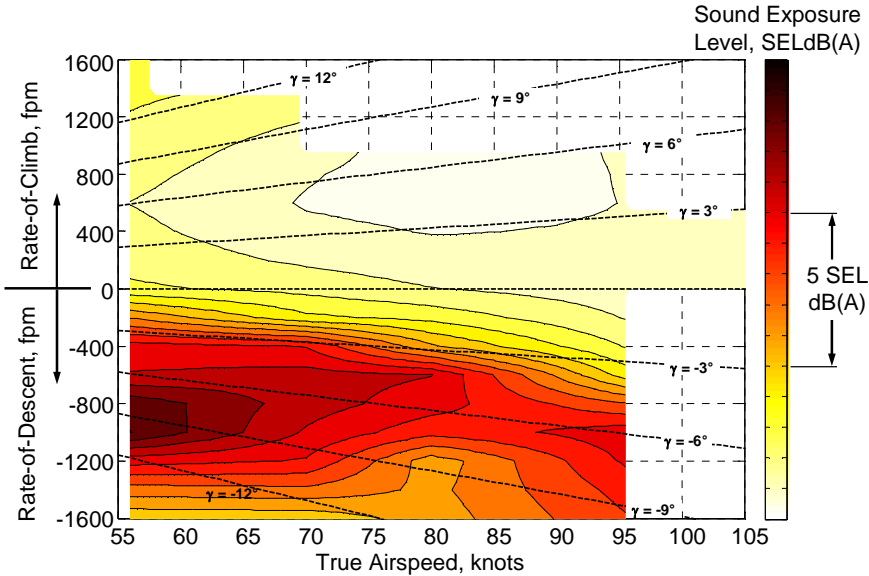
Figure 8. Sound exposure level at the centre microphone as a function of true airspeed and rate-of-descent/climb (contour lines are 1 SELdB(A) apart)

As the previous figure shows, using a time-integrated metric to represent the noise of the aircraft in the steady-state envelope slightly changes the conclusions. Indeed, it can be noticed that the high-noise region appearing at high speed and 1200 feet-per-minute (fpm) rate-of-descent in Figure 7 has now disappeared due to the time-integration factor. The climb condition minimum noise region has also been shifted to slightly higher airspeeds through the use of the SEL metric.

The directivity of rotorcraft noise in approach has been discussed extensively in the literature. In many approach flight conditions for example, the main rotor advancing side exhibits higher noise levels due to strong Blade-Vortex Interaction (BVI). Therefore, representing the ground acoustics of an aircraft in descent with only the centreline microphone does not provide all the necessary information for the design of low-noise procedures. In the next figure, the SEL rate-of-descent/climb vs. airspeed plot is shown once more, but with each point corresponding to the maximum SEL at any microphone location (shown on the same colour scale as Figure 8).
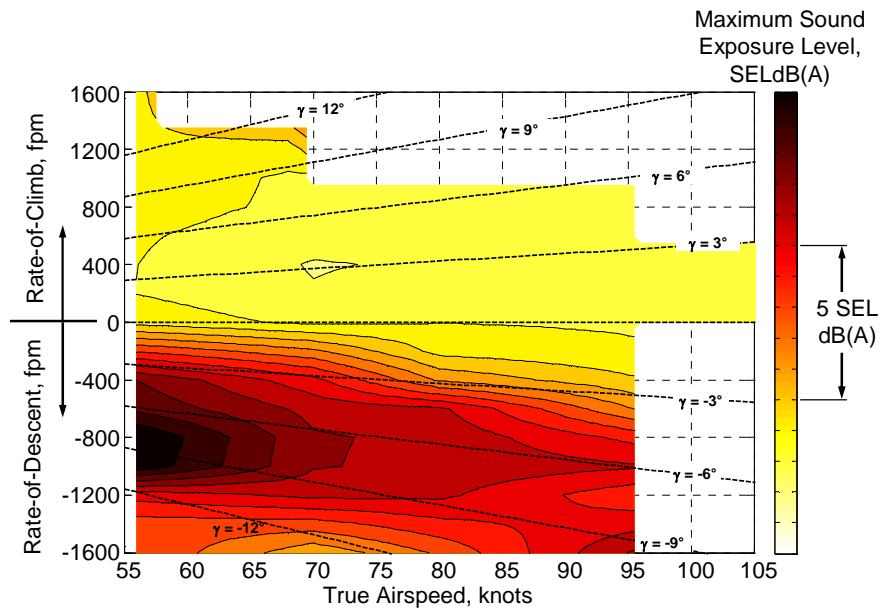
Figure 9. Maximum sound exposure level as a function of true airspeed and rate-of-descent/climb (contour lines are 1 SELdB(A) apart)

It can be seen from Figure 9 that the SEL rate-of-descent/climb vs. airspeed plot for the maximum of all microphones is similar to the same plot for the centreline microphone only (Figure 8). The high and low-noise regions are approximately in the same locations as for the centre microphone only. However, a noticeable difference must be noted. Using the maximum SEL, the low-noise region in approach is limited to 70 knots at 1600 fpm rate-of-descent. Using only the centreline microphone SEL (Figure 8), the low-noise approach region extends from 55 knots to 80 knots at 1600 fpm rate-of-descent. Therefore, the centre microphone data can be used to design low-noise flight profiles as a first estimate only. In order to take into account the important directivity of the impulsive approach noise sources, noise data at lateral microphones is necessary. Lateral noise data is also necessary to adapt low-noise procedures to the specific configuration of a takeoff or landing site.

5.2. Manoeuvring Flights

As mentioned above, the manoeuvring flights were performed over a grid array of 36 ground microphones. This array covered a large area of 780 m long by 580 m wide. However, a typical complete helicopter approach or takeoff procedure extends over many kilometres. Therefore, it is not practical to implement an array large enough to capture all phases of a complete flight with sufficient detail. For this reason, a segmented flight profile data acquisition methodology was used.

In this methodology, the manoeuvring segments are separated from the steady-state segments. For the approach, data was gathered for 'start-of-approach' manoeuvres and for 'end-of-approach' manoeuvres at different airspeeds and glideslopes. Using the data for steady-state flyovers and steady-state constant glideslope approaches, it is then possible to link the various segments and construct a suitable approximation to the desired complete profile. This greatly reduces the size of the required microphone array, and therefore reduces the test costs.

To illustrate this method, the case of a complete normal approach is presented below in Figure 10. The 'start-of-approach' manoeuvre segment begins in steady-state level flight at 110 knots, and then intercepts a 6° glideslope while decelerating to 70 knots. The SEL footprint

for this segment (measured using the 36-microphone grid array) is shown on the right hand side of the figure. It is followed by a steady-state descent segment at 6° and 70 knots. Two measured SEL lines are shown for this segment, corresponding to flights performed at 120 meters and 150 meters above the 9/11-microphone linear array. The last segment of the complete approach is the end-of-approach manoeuvre. It starts in a steady-state descent at 6° and 70 knots, then the glideslope is reduced and deceleration is applied to reach hover over the landing point. The measured SEL footprint for this segment is shown on the left of Figure 10. Note that the hover portion of the last segment is not taken into account in the computation of the SEL. A representative longitudinal trajectory is also shown on the figure for reference only (not to scale). The same colour scale is used to show the measured SEL footprints for each segment of the approach.
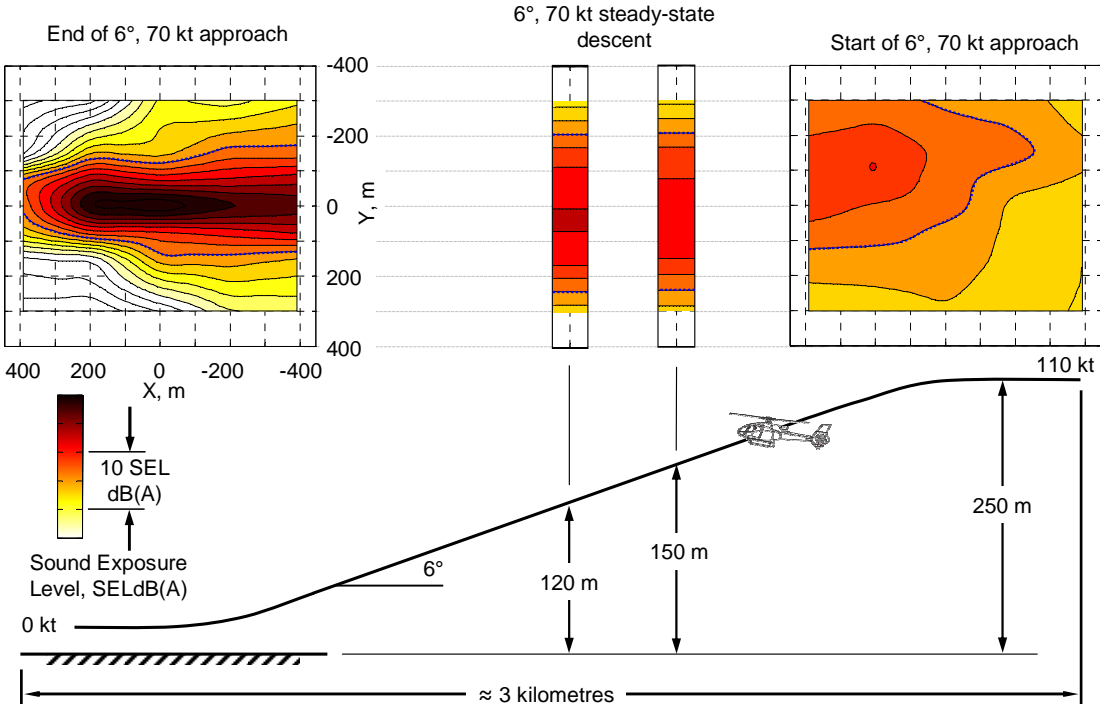
Figure 10. Acoustic footprint for a complete approach procedure reconstructed from 2 measured manoeuvring segments and 2 measured steady-state segments(contour lines are 2 SELdB(A) apart)

The previous figure illustrates the methodology used to construct a complete flight based on measured noise. If necessary, an interpolation can be used to join the various segments and obtain a complete footprint. Note that the information presented in Figure 10 could not have been obtained in a single flight due to the size of the microphone array (even though it is very extensive). For example, a noise increase can be seen on the right side of the helicopter at the start of the descent segment. This retreating side 'hotspot' (likely due to some form of main rotor interaction) could not have been captured without a dedicated 'start-of-approach' segment being performed over the microphone array.

To demonstrate the repeatability of the results as a function of microphone position, the following figure shows a sample 90-percent confidence interval SEL contour plot (as computed by the methodology of [9]). The footprint shown is for the 'start-of-approach' manoeuvre (as shown in Figure 10). Four runs of this flight condition are used to determine the confidence interval.

12
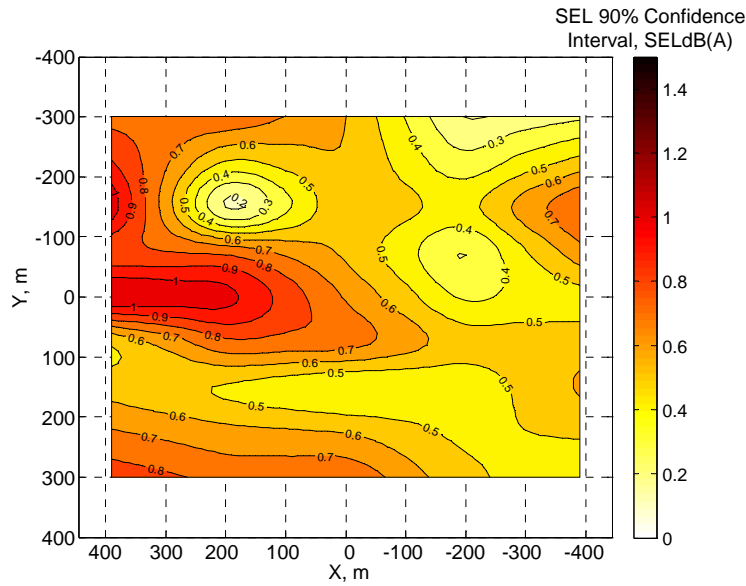
Figure 11. 90-percent confidence interval SEL footprint for 'start-of-approach' manoeuvre

As Figure 11 shows, the confidence interval is within the limit of +/- 1.5 SELdB(A) imposed by rotorcraft certification regulations. The area of decreased confidence mainly corresponds to the noise hotspot observed on Figure 10. This is expected, since the hotspot is located in the 'most unsteady' portion of the manoeuvre, and is highly dependent on pilot actions. However, this plot clearly shows that even a complex manoeuvre such as this one (involving a transition from level flight to a 6° descent and a deceleration from 110 knots to 70 knots), can be systematically performed with a good level of accuracy and repeatability with the use of a pilot guidance system.

As an example, Figure 12 shows the trajectory and groundspeed profile for a steep 'end-of-approach' manoeuvre starting at 58 knots. The parameters presented correspond to the average of four flights, and the 90-percent confidence interval is presented at various key positions along the trajectory.
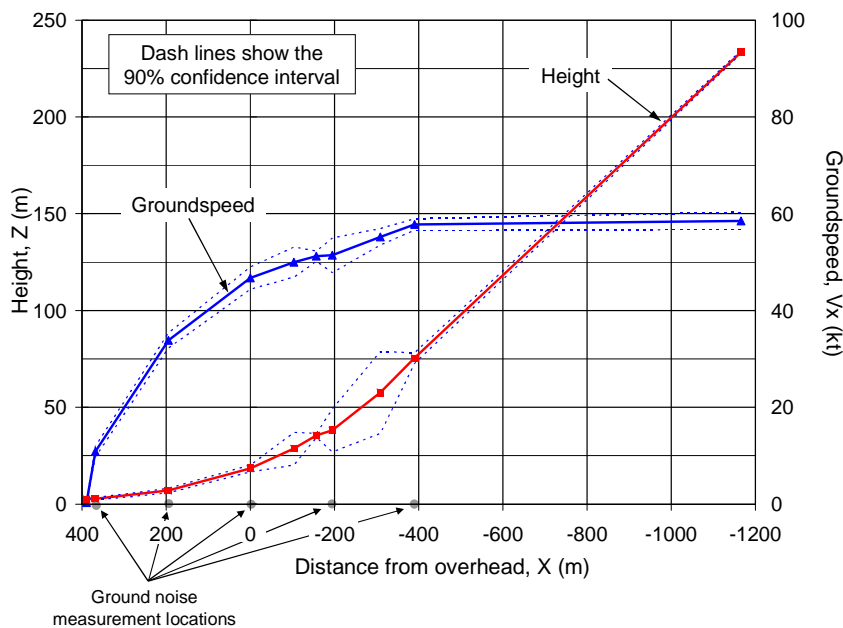
Figure 12. Trajectory and groundspeed profile for 58 knots steep 'end-of-approach' manoeuvre

13

Figure 12 shows that the groundspeed and height profiles exhibit a good degree of repeatability. The only segment with a large altitude variability is at the start of the transition (start of deceleration and rapid change in glideslope). High pilot workload during this segment causes this variability. This highlights the difficulty of implementing repeatable noise abatement procedures in real operations, with helicopters that are not equipped with a pilot guidance display.

6. CONCLUSIONS

This paper gives an overview of the EC130 B4 acoustic flight tests conducted through the Friendcopter research project. The test means, analysis methodology, and sample results were presented. In summary, the extensive testing and analysis equipment that were deployed for these campaigns lead to the successful characterization of the noise features of the aircraft throughout its normal operating flight envelope. In particular, the following points are important to acknowledge:

▪ In order to adequately represent the non-symmetrical lateral directivity of the EC130 B4, a minimum of 7 microphones should be used, covering 300 meters on each side of the aircraft. Additional microphones at lateral positions farther than 300 meters may also be necessary to model the long distance and low grazing angle propagation characteristics of a given aircraft.
▪ For the EC130 B4, a first approximation of the noise levels through the steady-state flight envelope can be obtained using only centreline microphone measurements. However, the full range of available lateral microphones should be used for the purpose of deriving noise abatement procedures.
▪ A low scatter was obtained in the trajectory and performance parameters, even for complex manoeuvres, showing that it is possible to perform noise abatement testing with strict trajectory tolerances. In this test, a pilot display showing the target trajectory and the associated tolerances was successful in providing repeatable flight profiles.
▪ The rigorous trajectory, performance, and meteorological tolerances ensured that the confidence interval on typical acoustic metrics obtained on both steady-state and manoeuvring flight was within the ICAO and FAA limits for all microphones.
▪ The acoustic database now available for the EC130 B4 is extensive, and will be used to design noise abatement flight profiles. The data will also serve as the input to the HELENA acoustic footprint prediction software being developed as part of the Friendcopter project.
▪ A novel methodology was introduced to acquire manoeuvring data and reconstruct footprints for complete flight profiles. This methodology provides a way to reduce flight test costs while emphasising the acquisition of quality data. The resulting database can be used to design low-noise profiles and gain an understanding of the complex acoustics characteristics of realistic flight manoeuvres.

These points must be taken into account in the preparation of future noise abatement flight tests, as well as in the development of guidance for the gathering and correction of data for land use planning purposes.

ACKNOWLEDGMENTS

REFERENCES

[1]   Allongue, M., Marze, H.J., Potdevin, F., "The Quiet Helicopter: From Research to Reality," Presented at the American Helicopter Society 55th Annual Forum, Montreal, Canada, May 1999.

[2]   Hawles, D. R., "Flight Operations to Minimize Noise," Presented at the American Helicopter Society-AIAA-University of Texas at Arlington Joint Symposium on Environmental Effects of VTOL Designs, Arlington, Texas, Nov 16-18, 1970, and Vertiflite, Feb. 1971.

[3]   Jacobs, E.W., Prillwitz, R.D, Chen, R.T.N., Hindson, W.S., and Maria, O.L.S., "The development and flight test demonstration of noise abatement approach procedures for the Sikorsky S-76," Presented at the American Helicopter Society Technical Specialists' Meeting for Rotorcraft Acoustics and Aerodynamics, Williamsburg, VA, Oct. 1997.

[4]   Janakiram, R. D.; O´Connell, J. M.; Fredrickson, D. E.; Conner, D. A. and Rutledge, C. K., "Development and Demonstration of Noise Abatement Approach Flight Operations for a Light Twin-engine Helicopter – MD Explorer", Presented at the American Helicopter Society Technical Specialists' Meeting for Rotorcraft Acoustics and Aerodynamics, Williamsburg, VA, Oct. 1997.

[5]   Conner, D.A., Edwards, B.D., Decker, W.A., Marcolini, M.A., and Klein, P.D., "NASA/Army/Bell XV-15 Tiltrotor Low Noise Terminal Area Operations Flight Research Program," AIAA/CEAS 6th Aeroacoustics Conference, Lahaina, HI, June 2000.

[6]   Schmitz, F. H., Gopalan, G., Sim, B. W., "Flight Path Management and Control Methodology to Reduce Helicopter Blade-Vortex Interaction (BVI) Noise", Journal of Aircraft, Vol. 39, No. 2, pp. 193-205, March-April, 2002.

[7]   Gervais, M., Schmitz, F. H., "Tiltrotor BVI Noise Reduction Through Flight Trajectory Management & Configuration Control," Journal of the American Helicopter Society, Vol. 49, (4), Oct. 2004, pp. 436-446.

[8]   Yin, J., Spiegel, P., Bucholz, H., Pierre Spiegel, Heino Buchholz, "Towards Noise Abatement Flight Procedure Design: DLR Rotorcraft Noise Ground Footprints Model and its Validation," Presented at the 30th European Rotorcraft Forum, Marseille, France, Sept. 2004.

[9]   International Civil Aviation Organization, "Environmental Protection, Volume 1: Aircraft Noise," Fourth Edition, Amendment 8, International Standards and Recommended Practices, Annex 16 to the Convention on International Civil Aviation, Montreal, Canada, July 2005.

[10] Federal Aviation Administration, "Federal Aviation Regulations Part 36 - Noise Standards: Aircraft Type and Airworthiness Certification," Amendment 36-27, Washington, D.C., Sept. 2005.

[11] International Civil Aviation Organization, "Environmental Technical Manual on the Use of Procedures in the Noise Certification of Aircraft," Third Edition, April 2007.

[12] Bernardini, G., Serafini, J., Iannniello, S., Gennaretti, M, "Aeroelastic Modeling Effect in Rotor BVI Noise Prediction," AIAA paper 2006-2606, Presented at the 12th AIAA/CEAS Aeroacoustics Conference, Cambridge, MA, May 2006.

[13] Bernardini, G., Gennaretti, M., Brouwer, H., Hounjet, M., Drikakis, D, Kokkalis, A., Loiodice, S., Perez, G., Ponza, R., "Assessment of Computational Tools for the Prediction of BVI noise," Presented at the 32nd European Rotorcraft Forum, The Netherlands, Sept. 2006.

[14] Sim, B.W., Schmitz, F.H., Beasman, T., "Blade-Vortex Interaction (BVI) Noise of Helicopters Operating In Horizontal Wind Shear," Presented at the American Helicopter Society 61th Annual Forum, Grapevine, TX, May 2005.